Dependence of energy gap on x and T in $Zn_{1-x}Mn_xSe$: The role of exchange interaction

R. B. Bylsma, W. M. Becker, J. Kossut,* and U. Debska
Physics Department, Purdue University, West Lafayette, Indiana 47907

D. Yoder-Short
Physics Department, Michigan Technological University, Houghton, Michigan 49931
(Received 13 January 1986)

Photoluminescence and reflectivity measurements have been carried out on $Zn_{1-x}Mn_xSe$ solid solutions in the complete range of crystal compositions, $0 \le x \le 0.55$. The features of the photoluminescence and reflectivity data near the band edge enabled us to determine values of the fundamental band gap as a function of Mn molar fraction x and temperature ($8\ K \le T \le 300\ K$). The energy gap in crystals with compositions in the vicinity of the zinc-blende–wurtzite structural transition ($0.2 \lesssim x \lesssim 0.3$) exhibited a scatter of values, probably associated with the presence of various polytypes (as evidenced by transmission-electron-microscopy measurements). The dependence of E_g on x is anomalous for $0 \le x \le 0.2$, showing a *minimum* in the E_g vs x curve. A simple model (in terms of second-order perturbation theory in s-d and p-d interactions) relates this minimum to a maximum observed in the magnetic susceptibility as a function of x. For samples with $x \gtrsim 0.35$, the E_g dependence on T shows an onset of an additional blue shift as the temperature is lowered below ~ 150 K. This onset, though not reproduced by our simple calculation, appears to be also related to the presence of s-d and p-d interactions.

I. INTRODUCTION

Currently much interest is focused on a class of materials known as diluted magnetic semiconductors (DMS).[1] These materials are II-VI binary compounds in which a magnetic ion, usually Mn^{2+}, is substitutionally incorporated in the host crystal in place of the group-II element. The resulting crystals have interesting optical and magneto-optical properties, including a compositionally and magnetically tunable band gap. $Zn_{1-x}Mn_xSe$ is a wide-band-gap DMS whose properties are relatively unexplored. Recently, successful growth of good optical quality crystals of this alloy has been achieved.[2] In an earlier study of optical properties of this alloy system,[3] the energy gap was determined only for materials of low Mn concentrations ($x \le 0.103$). Here we investigate samples spanning the range from $x = 0.0$ to 0.55, and explore the dependence of the gap both on x and T.

Usually, one observes a nearly linear dependence of energy gap E_g on x and a blue shift of the gap with decreasing T. This blue shift is linear in T for high T and proportional to T^2 for low T.[4] In the course of this investigation, two anomalous behaviors of E_g in $Zn_{1-x}Mn_xSe$ were observed. The first was a distinct initial decrease in E_g at low x, an effect consistent with previous observations by Twardowski *et al.*[3] The magnitude of this decrease was found to be temperature dependent. The second anomaly, observed in crystals with high Mn concentration, was the onset of an additional blue shift of the band-edge photoluminescence (PL) at low temperatures. Such shifts have been noted previously in other DMS,[5–7] but not reported for $Zn_{1-x}Mn_xSe$. It is known that the s-d and p-d exchange interactions are important in DMS materials and strongly modify the energy of band states in the presence of a magnetic field. We propose that the observed anomalous behaviors mentioned above are in part attributable to these exchange interactions, even in the absence of applied magnetic field. In particular, we show that for low x there is a correlation between the measured magnetic susceptibility and the deviation of E_g from a linear dependence on x.

The first work on solid solutions of $Zn_{1-x}Mn_xSe$ indicated that they crystallize in the zinc-blende structure for $x \le 0.35$ and in the wurtzite structure for $0.35 \le x \le 0.50$.[8] Recently, the range over which $Zn_{1-x}Mn_xSe$ crystals can be grown has been extended to $x = 0.57$.[2] This work also revealed that the transition from cubic to hexagonal $Zn_{1-x}Mn_xSe$ is not abrupt. Since the zinc-blende to wurtzite phase transition involves only small changes in free energy, more complicated structures such as microtwins, polytypes, etc. may be expected near the phase boundary. Indeed, from x-ray powder diffraction spectra[2] there is evidence of hexagonal reflections for x as low as 0.19. Our work shows that polytypism must be taken into account in the study of the optical properties for $0.20 \le x \le 0.3$. For $x \ge 0.34$, the x-ray data give no evidence of cubic regions in the crystals. Here we were able to correlate structural changes with variations in the band gap over the complete range of solid solution.

In Sec. II a description of the experimental methods and equipment is given. The results are presented in Sec. III. We discuss various aspects of the results in Secs. IV and V. Included in Sec. IV is an explanation of the nonsystematic dependence of the fundamental gap on x in the region of the structural phase transition based on the effects of polytypism. In Sec. V we analyze the anomalous behaviors seen in the dependence of the gap on x and T in terms of the s-d and p-d exchange interaction.

II. EXPERIMENTAL

The crystals used in this study were grown by the Bridgman method,[2] and the Mn concentrations of all samples were established by electron microprobe analysis. The crystal structure of selected samples was determined by x-ray powder diffraction measurements and has been reported elsewhere.[2] The samples investigated are listed in Table I. Band-gap energies appearing in the table were taken from our PL and reflectivity data.

The excitation source for PL measurements was an argon-ion laser operated in the uv (351.1- and 363.8-nm lines). Typical incident power was ~ 10 mW focused to a spot approximately 100 μm in diameter. Crystals were mounted strain free in a Dewar with temperature-controlling capabilities, allowing measurements to be made from 5 to 300 K. The detection system consisted of a 0.22-m Spex double grating monochromator, with an RCA 31034 photomultiplier tube connected to a photon counting system. The majority of the samples were freshly cleaved; the remainder were polished, or polished and etched. PL results were essentially independent of sample preparation.

Reflection spectra were made in a backscattering configuration. The incident light was selected from a 150-W xenon arc lamp by a $\frac{1}{4}$-m grating monochromator. Reflected light intensity was measured with an IP28 photomultiplier tube. A computerized data acquisition system allowed extraction of the reflectivity feature from a large background. All the reflectivity measurements were performed on freshly cleaved surfaces.

III. RESULTS

A. Photoluminescence

In Fig. 1 are presented the PL spectra of $Zn_{1-x}Mn_xSe$ for concentrations from $x=0.0$ to 0.554 taken at 6.5 K. The spectrum of pure ZnSe (shown in Fig. 2) is typical of those seen by other investigators.[9,10] For example, at

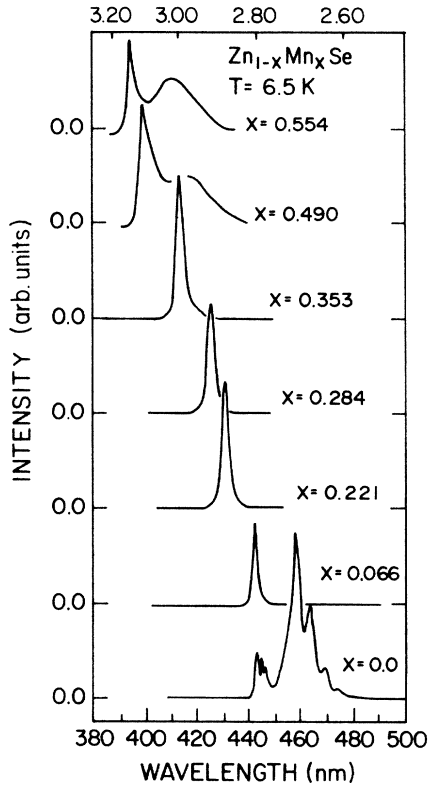

FIG. 1. PL spectra of $Zn_{1-x}Mn_xSe$ for $x=0.00$ to 0.554 at 6.5 K.

2.798 eV there are at least three unresolved peaks. We assign these to various donor-bound excitons, consistent with Dean *et al.*[11] There is also structure at 2.784 eV; such structure has been previously ascribed to acceptor-bound excitons.[12] The commonly observed "near-edge" emission is dominated by a peak at 2.704 eV and followed by vibronically coupled sidebands. This emission has been attributed to transitions involving holes bound to acceptors and either free electrons or electrons bound to

TABLE I. Concentration of Mn ions, x from electron microprobe analysis and energies of PL peaks and reflectivity maxima at 6.5 and 77 K for studied samples. Feature energies are in eV and FWHM are in meV.

Crystal symbol	x	E_{PL}	FWHM 6.5 K	E_{refl}	E_{PL}	FWHM 77 K	E_{refl}
P65A	0.0	2.798	10.7	2.782	2.792		2.773
P27	0.066	2.796	15.8	2.790	2.783	21.8	2.773
P103	0.221	2.876	20.7		2.852	25.8	
P36	0.229	2.919	22.0	2.881	2.863	25.1	2.846
P103A	0.260	2.866	17.8	2.849	2.839	17.6	2.816
P103D	0.284	2.912	21.9	2.889	2.889	29.6	2.864
P54	0.303	2.989	22.3		2.945	27.9	
P108B	0.353	2.998	23.9		2.949	23.1	
P108T	0.360	3.006	22.6	2.997			2.953
P52	0.394	3.058	28.6		3.009	53.7	
P79	0.482	3.090	39.8	3.091	3.039	48.1	3.042
P60	0.490	3.105	46.4		3.039	73.8	
P68B	0.554	3.147	47.0	3.128	3.075	75.2	3.089

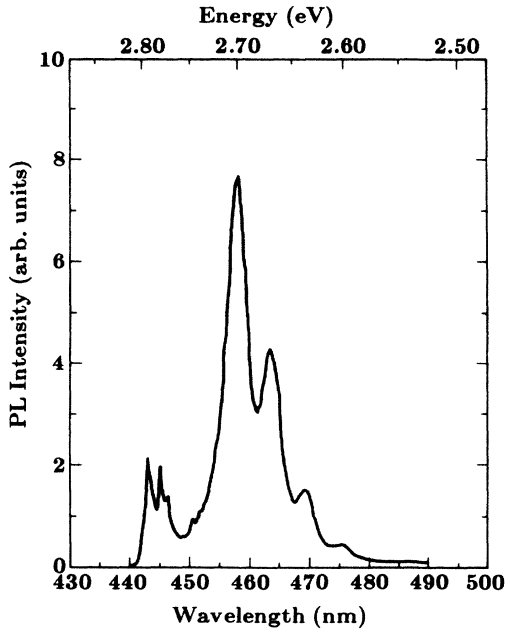

FIG. 2. Details of PL spectra in ZnSe at 6.5 K.

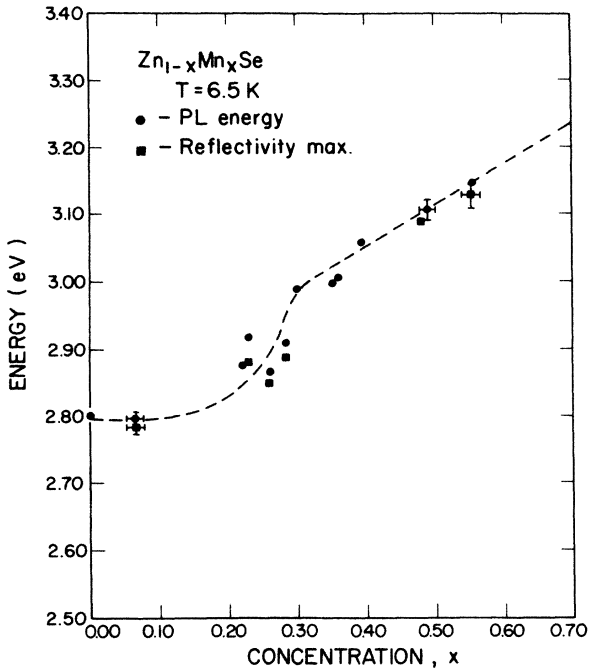

FIG. 3. Energy versus Mn mole fraction x in $Zn_{1-x}Mn_xSe$ of the band-edge photoluminescence peak (●) and reflectivity maximum (■) at 6.5 K.

donors.[9] An LO-phonon energy of 31.8 meV is derived from the sideband spacing, in agreement with the published value.[9] Here, being most concerned with the determination of the energy gap, we take the highest energy feature as a good measure of the E_g.

At $x=0.066$ the band-edge PL consists of only one peak; this peak is slightly red shifted from the highest energy feature seen in pure ZnSe. With the incorporation of still more Mn, the band-edge PL broadens and becomes less intense. At 6.5 K the full width at half maximum (FWHM) of the band-edge PL varies from ~ 15 meV for $x=0.066$ to ~ 47 meV for $x=0.554$. For $x \geq 0.4$, a broad band begins to appear at ~ 3.0 eV. This emission below the band gap is unexpected and as yet unidentified. Measurements show that there is no noticeable (± 10 meV) thermal shift of this band up to 60 K, although the band-edge PL is shifted to lower energy by ~ 40 meV in the same temperature range. Thus, this emission does not appear to be related to the valence-to-conduction-band energy difference. We note that all Mn^{2+}-related intra-ionic emissions lie at much lower energy ($h\nu \lesssim 2.1$ eV) than the energy range discussed here.

Although the general trend of the band-edge PL energy is an increase with increasing Mn concentration, there is a deviation from this trend at $x=0.066$. Figure 3 shows this nonmonotonic dependence of band-edge PL energy on Mn concentration. This is consistent with the reflectivity results of Twardowski *et al.*[3] on crystals with $x \leq 0.103$. Such an effect is unusual, since the minimum of the E_g versus x curve is localized at low x (even after the linear part has been subtracted). Moreover, a strong temperature dependence of both the position and the depth of the minimum is noted. These two facts do not allow an interpretation in terms of band-gap bowing.[13] There is notable scatter in the data points for $0.20 < x < 0.30$. An analysis shows that this cannot be attributed solely to uncertainties

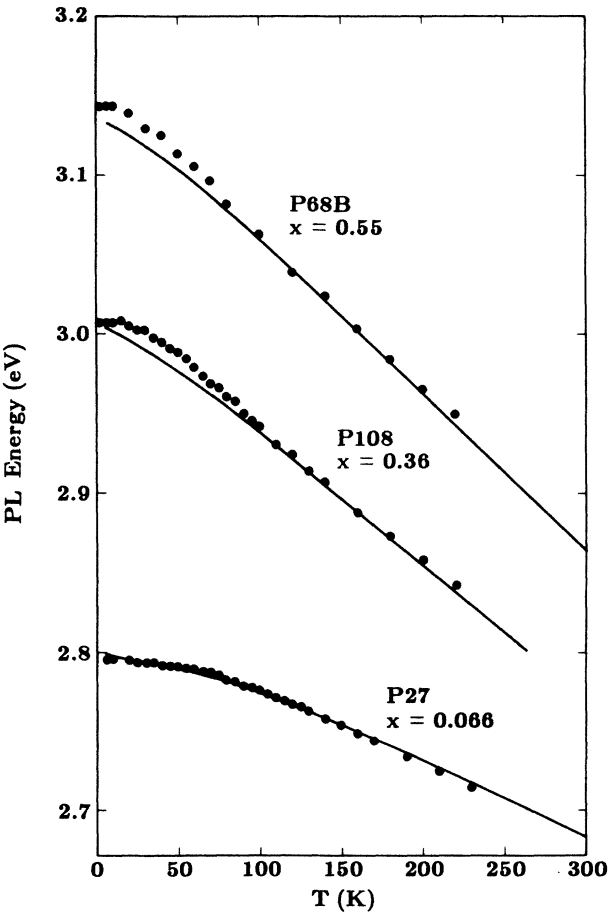

FIG. 4. Temperature dependence of PL peak for three Mn concentrations. The lines are theoretical fits using Eq. (12) and the parameters in Table III.

in concentration determination; the source of scatter will be explained in Sec. IV. Above $x=0.30$ the dependence of E_g on x appears linear. Measurements taken at 77 K of the band-edge PL reveal the same trends (i.e., nonlinearities, scatter in data, etc.) as at 6.5 K. The respective positions are, however, shifted to lower energy, reflecting the narrowing of the band gap with increasing temperature.

Photoluminescence measurements of the band-edge feature for three of these samples were made over a temperature range from 6.5 to 250 K. The results presented in Fig. 4 demonstrate that at high temperatures a linear closure of the band gap with temperature occurs, the rate of closure depending on Mn concentration. A deviation from the normal semiconductor behavior[4] is present at low temperatures in samples with high Mn mole fraction: an extra blue shift of the band edge with decreasing temperature is seen. The amount of this blue shift also appears to be dependent on the Mn concentration. Both this effect and the nonlinearity of E_g versus x for $x \leq 0.15$ are discussed in Sec. V in terms of the s-d and p-d exchange interaction.

B. Reflectivity

Reflectivity measurements were undertaken in order to confirm the band-edge energies established in PL, in particular, the scatter of the PL data in the range $0.20 \leq x \leq 0.30$. Figure 5 shows the near-band-edge reflectivity spectra over the entire range $0.0 \leq x \leq 0.554$. The reflectivity feature seen by us in pure ZnSe is identical in both energy position and shape to published spectra.[14] In the $x=0.066$ sample only a peak with a sharp high-energy cutoff is seen. The peak becomes broader with increasing Mn concentration; at the highest concentration ($x=0.554$) only a step remains. The energies of the reflectivity peaks (see Fig. 3) were found to be in agreement with the band-edge PL energies (see Table I) for both 6.5 and 77 K. There is a small, but systematic, shift of the reflectivity-derived points toward lower energies as compared to the PL emission maxima. From Fig. 5 it can be seen that agreement would be improved if E_g were deduced from a point on the high-energy side of the reflectivity feature. Overall this agreement confirms the band-edge energies determined by PL measurements, particularly in the region from $x=0.20$ to 0.30 where the aforementioned unexplained scatter in the data occurs.

It is important to know the relationship between energy positions of PL and reflectivity features and the actual value of the energy gap. Photoluminescence and reflectivity measurements do not necessarily pinpoint the position of the free exciton. Absorption measurements by Morales *et al.* on an ~ 7.8-μm-thick $Zn_{1-x}Mn_xSe$ ($x \cong 0.50$) crystal achieved transmission up to 3.14 eV at liquid-helium temperatures without detecting any structure attributable to excitations.[15] This energy represents a lower bound on a possible free-exciton position (slightly higher than the PL energy observed for this composition). The near-band-edge PL in $Zn_{1-x}Mn_xSe$ is similar in nature to that seen in alloys of $Cd_{1-x}Mn_xTe$ in that it is featureless and becomes broader and weaker with increasing concentration. In our analysis, we assume that the PL maxima are due to bound states near the band edge, with binding energies independent of concentration.

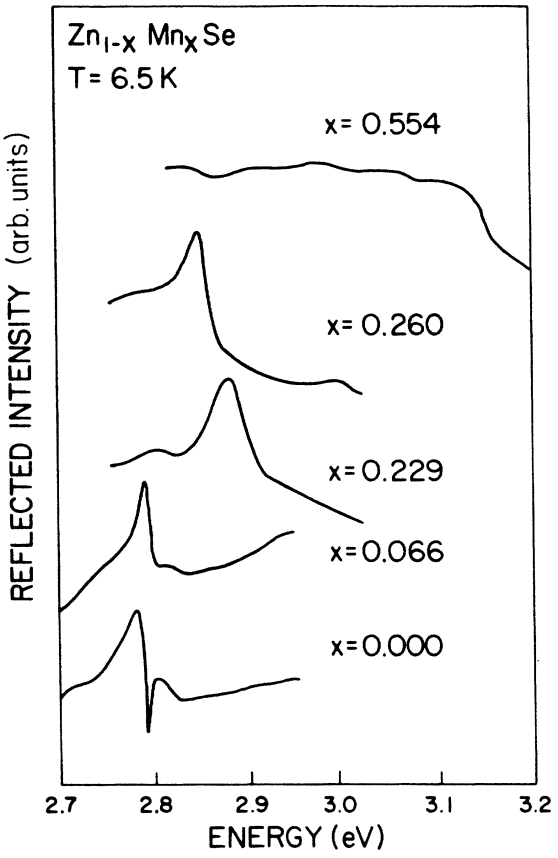

FIG. 5. Reflectivity spectra of $Zn_{1-x}Mn_xSe$ crystals at 6.5 K.

IV. INFLUENCE OF STRUCTURAL PHASE TRANSITION

As mentioned above, in the concentration range from $x=0.20$ to 0.30 there is some scatter in the data which cannot be accounted for by concentration uncertainties. We suggest that this scatter is related to the presence of both zinc-blende and wurtzite phases in crystals with compositions lying close to the structural phase transition ($x \sim 0.3$).

The work of Brafman and Steinberger[16] on polytypes of ZnS shows that the absorption edge of hexagonal crystals is displaced from that of cubic crystals. They determined the percentage of hexagonality (α) and related this quantity to absorption edges in various ZnS crystals. For zinc blende $\alpha=0$ and for completely wurtzite crystals $\alpha=1$. As α increased from $\alpha=0$ to $\alpha=1$, those authors found an upward energy shift in the absorption edge of 105 and 71 meV for incident photons polarized parallel and perpendicular to the wurtzite c axis, respectively. These measurements showed that the energy variation is linearly dependent on α. Calculations by Birman[17] qualitatively predicted such an energy shift. His results using the linear-combinations-of-atomic-orbitals method showed

that at the zone center, $\mathbf{k}=\mathbf{0}$, in a wurtzite crystal the lowest conduction band shifts up in energy compared to a zinc-blende crystal, and the highest valence band splits into two components. Birman also suggested that this calculation might also apply to randomly faulted crystals, structures in which the layers of zinc blende and wurtzite occur in a random manner. In this case the perturbation potential $V'(\alpha)$ which causes the shifting and splitting of states between zinc-blende and wurtzite crystals would be a function of α. The results of Brafman and Steinberger indicate that $V'(\alpha)$ is proportional to α, i.e., $V'(\alpha)=V'_0\alpha$. Assuming that such a V'_0 can be defined for $Zn_{1-x}Mn_xSe$ crystals and that it is of the order of ~ 60 meV, which is the difference between energy gaps in zinc-blende and wurtzite forms of ZnSe,[18] then a change in α of ~ 0.5 would give the absorption-edge shift of the order of the scatter observed by us.

To further investigate this possibility, five randomly selected pieces of each of the four crystals in the $0.20<x<0.30$ range were examined for polytypism by means of electron diffraction and scanning electron microscopy. The results are listed in Table II. In the polytype designation mH, m represents the periodicity of the polytype and H denotes the hexagonal structure. For example, with $m=4$, i.e., $4H$, and the three possible close-packed stacking planes labeled A, B, and C, the stacking will be $ABACABAC\ldots$. An hexagonal structure ($2H$) has $ABABAB\ldots$ stacking and in a cubic structure ($3C$) the stacking follows the formula $ABCABC\ldots$. In the case of the $4H$ polytype, $\alpha=0.5$ since 50% of the layers, namely, the B and C layers, are in hexagonal environment. The stacking sequence for $m\geq 6$ can be of many forms and the percentage of hexagonality can be known only by determining the exact stacking order. The determination for the samples which consisted of $8H$ polytypes was not attempted.

As can be seen in Table II, crystals P36 and P103 were found to contain both $4H$ and $8H$ polytypes. In crystal P103D only $4H$ polytypes were seen; crystal P103A was found to be cubic with many microtwins. This establishes that polytypes are indeed possible in this concentration range. It also indicates that the type of polymorphism is not predictable by determination of sample concentrations only. Most importantly it offers an explanation for the nonsystematic behavior of E_g with x as measured by PL and reflectivity. A comparison of P103A ($x=0.260$) and P103D ($x=0.284$) shows that they have $\alpha=0.00$ and 0.50, respectively. This difference would cause the band edge of P103A to be red shifted relative to the band edge of P103D by approximately $V'_0/2$. We observe a red shift of ~ 45 meV at 6.5 K. Assuming that the perturbation potential for $Zn_{1-x}Mn_xSe$ is of the same order of magnitude as that of ZnSe, the band-gap energy difference is correct to within the uncertainties of the measurements.

Above the region of crystal structure transition, both PL and reflectivity data allow one to extrapolate E_g to $x=1.0$, that is, to MnSe in the hypothetical wurtzite structure. This extrapolation gives ~ 3.4 eV (6.5 K) and ~ 3.3 eV (77 K). These values are within 50 meV of what would be expected from measurements on $Cd_{1-x}Mn_xSe$.[19] A value of 3.4 eV for the band gap of zinc-blende MnSe was also obtained by L.A. Kolodziejski *et al.* from measurements on zinc-blende molecular-beam-epitaxy (MBE)-grown epilayers of $Zn_{1-x}Mn_xSe$.[20]

V. BAND GAP VERSUS x AND T: ROLE OF EXCHANGE INTERACTION

As can be seen from Fig. 3, the dependence of band-edge PL energy on x shows anomalous behavior at low x, namely, there is an initial decrease in energy followed at higher concentration by an increase. Only for concentrations above $x\simeq 0.30$ does a linear dependence of PL energy on x appear to occur. The initial drop in energy at low concentrations is consistent with previous results.[3] This unusual behavior has also been seen in $Cd_{1-x}Mn_xS$ by Ikeda *et al.*[21] Those authors found that their data could not be explained on the basis of a broadening and shifting of energy levels due to statistical fluctuations of the crystal potential in an alloy (band-gap bowing).

In this section, we argue that the anomalous behavior of E_g versus x and T, after the removal of the polytypism-related scatter, is due to s-d and p-d exchange interactions. A strong exchange interaction is known to occur in DMS materials between the d electrons of the Mn ions and the band electrons, and is responsible for large-g factors observed in these alloys. This interaction and the parameters describing it have been measured in various DMS materials. In $Zn_{1-x}Mn_xSe$ such measurements have been made by Twardowski *et al.*[3] and Heiman *et al.*[22] The exchange constant involving the valence band in this material is relatively large ($\beta=1.22$ eV), i.e., we may expect the exchange-interaction-related phenomena to be quite strong and pronounced. An analysis of the effect this interaction has on the band gaps of magnetic semiconductors has been made by other authors,[23,24] using

TABLE II. Results of determination by TEM of structural polytypes in $Zn_{1-x}Mn_xSe$ crystals with $0.20<x<0.30$. The notation is described in the text.

Crystal symbol	x	Sample no. 1	2	3	4	5
P103	0.221	$4H$	$4H$	$8H$	$8H$	
P36	0.229	$8H$	$4H$	$8H$	$8H$	$8H$
P103A	0.260	$3C$	$3C$	$3C$	$3C$	$3C$
P103D	0.284	$4H$	$4H$	$4H$	$4H$	$4H$

second-order perturbation theory. This analysis has also been extended to $Cd_{1-x}Mn_xTe$ to explain the temperature behavior of band-gap variation with temperature in the composition regime in which a phase change occurs between paramagnetic and antiferromagnetic ordering.[5] We have rederived the formula in question to account for the fourfold degeneracy of the valence band. The following treatment expresses the result in terms of empirically obtained magnetic susceptibilities, in order that qualitative models of spin-spin correlation functions need not be relied upon, as was the case in Ref. 5.

A. Theoretical background

The Hamiltonian describing the coupling of band electrons and localized Mn spins is taken as

$$H=\sum_n J(\mathbf{r}-\mathbf{R}_n)\mathbf{s}\cdot\mathbf{S}_n \ , \tag{1}$$

where $J(\mathbf{r}-\mathbf{R}_n)$ is the exchange integral for an electron with spin $\mathbf{s}$ at $\mathbf{r}$ and a magnetic ion with spin $\mathbf{S}_n$ at $\mathbf{R}_n$. The unperturbed band states are, in the case of the conduction band, given by

$$V^{-1/2}\exp(i\mathbf{kr})\phi_s\uparrow(\downarrow) \ ,$$

where V is the volume of the crystal, ϕ_s is the simple periodic Bloch amplitude, and $\uparrow(\downarrow)$ denote the spin part of the wave functions. In the case of the valence bands, the periodic part is taken as appropriate $p(\Gamma_8)$-like functions.[25] The eigenenergies for the conduction, heavy-hole, and light-hole bands are approximated by $E_c^{(0)}=\hbar^2k^2/2m_c$, $E_{hh}^{(0)}=-E_{0g}(x)-(\hbar^2k^2/2m_{hh})$, and $E_{lh}^{(0)}=-E_{0g}(x)-(\hbar^2k^2/2m_{lh})$, respectively, where m_c, m_{hh}, and m_{lh} are effective masses for the conduction electrons, heavy holes, and light holes, respectively. Thus, the nonparabolicity in the valence band is neglected in our simple approach. The energy gap $E_{0g}(x)$ will be assumed to be a linear function of the alloy concentration in the spirit of the simplest virtual-crystal approximation.

Carrying out the calculation of the first-order energy correction due to the perturbation given by Eq. (1), one finds that the correction is proportional to $\langle S_z\rangle$, where $\langle S_z\rangle$ is the thermal average of S_z. In the absence of a magnetic field $\langle S_z\rangle=0$; therefore, there is no contribution to the energy gap from first-order perturbation theory, except for ferrimagnets and ferromagnets, which does not apply in our case.

The correction for the conduction band due to second-order perturbation theory is given by

$$E_c^{(2)}=\frac{1}{4V}\frac{\Omega_0^2}{8\pi^3}\sum_{m,n}\int d^3k'\,\alpha^2(\mathbf{k}-\mathbf{k}')\frac{S_m^zS_n^z+S_m^+S_n^-}{E_k-E_{k'}} \times e^{i(\mathbf{k}-\mathbf{k}')\cdot(\mathbf{R}_m-\mathbf{R}_n)} \ , \tag{2}$$

where Ω_0 is the unit-cell volume,

$$\Omega_0\alpha(\mathbf{k}-\mathbf{k}')=\int d^3r\,e^{i(\mathbf{k}-\mathbf{k}')\cdot\mathbf{r}}J(r)\,|\,\phi_s(r)\,|^2 \ ,$$

and $S_n^{\pm}=S_n^x\pm iS_n^y$. There is no spin splitting, rather the perturbation results in a rigid shift of the bands. With the magnetic susceptibilities defined as follows ($\mu,\nu=x,y,z$; $\mathbf{q}=\mathbf{k}-\mathbf{k}'$):

$$\chi^{\mu\nu}(\mathbf{q})=\frac{1}{V}\frac{(g\mu_B)^2}{k_BT}\sum_{m,n}e^{[i\mathbf{q}\cdot(\mathbf{R}_n-\mathbf{R}_m)]} \times(\langle S_n^\mu S_m^\nu\rangle-\langle S_n^\mu\rangle\langle S_m^\nu\rangle) \ , \tag{3}$$

and assuming again $\langle S_n^\mu\rangle=0$ ($\chi^z=\chi^{zz}$, $\chi_\perp=\chi^{xx}=\chi^{yy}$) we obtain

$$[\chi^z(q)+2\chi_\perp(q)]\frac{k_BT}{(g\mu_B)^2} =\frac{1}{V}\sum_{m,n}(\langle S_m^zS_n^z\rangle+\langle S_m^+S_n^-\rangle)e^{i\mathbf{q}(\mathbf{R}_m-\mathbf{R}_n)} \ . \tag{4}$$

We can now express the energy correction due to the exchange interaction in terms of magnetic susceptibility values which can be taken from an independent experiment. We also assume that

$$\alpha(q)=\begin{cases}\alpha & \text{for } q\le q_0 \ ,\\ 0, & q>q_0 \ .\end{cases} \tag{5}$$

The above assumption is valid based on the short-ranged nature of $J(r)$ (Ref. 23) and leaves the cutoff q_0 as a free parameter which will be determined from the data. Furthermore, it is expected that in a disordered spin system $\chi^{\mu\nu}(q)$ will be q independent. This is certainly true when the spins are in a randomly distributed and oriented state as is the case with the paramagnetic phase. With these conditions, the correction to the energy of the bottom of the conduction band ($k=0$) is

$$E_c^{(2)}(k=0)=-\frac{m_cq_0}{\pi^2\hbar^2}\left[\frac{\alpha\Omega_0}{2}\right]^2\frac{k_BT}{(g\mu_B)^2}(\chi_z+2\chi_\perp) \ . \tag{6}$$

Similarly for the valence bands, the second-order correction can be derived with the assumption that β—the exchange parameter involving p-like states—depends on q in a fashion analogous to Eq. (5), and χ is q independent, the result for $\mathbf{H}=0$ and $\mathbf{k}=0$ is

$$E_{hh}^{(2)}=\frac{m_{hh}q_0}{\pi^2\hbar^2}\left[\frac{\beta\Omega_0}{2}\right]^2\frac{k_BT}{(g\mu_B)^2}\left[\chi_z+\frac{2}{3}\frac{m_{lh}}{m_{hh}}\chi_\perp\right] \ , \tag{7}$$

and

$$E_{lh}^{(2)}=\frac{m_{lh}q_0}{\pi^2\hbar^2}\left[\frac{\beta\Omega_0}{2}\right]^2\frac{k_BT}{(g\mu_B)^2} \times\left[\frac{1}{9}\chi_z+\frac{8}{3}\chi_\perp+\frac{2}{3}\frac{m_{lh}}{m_{hh}}\chi_\perp\right] \ . \tag{8}$$

Again, a rigid shift of the valence bands occurs; however, there is a splitting of the heavy-hole and light-hole bands at $k=0$ induced by the p-d interaction. By taking the difference of Eqs. (6) and (7) we may express the band gap as

$$E_g(x,T)=E_{0g}(x,T)-\left[\frac{\Omega_0}{2}\right]^2\frac{k_BT}{(g\mu_B)^2}\frac{q_0}{\pi^2\hbar^2} \times\chi[3m_c\alpha^2+(m_{hh}+\tfrac{2}{3}m_{lh})\beta^2] \ . \tag{9}$$

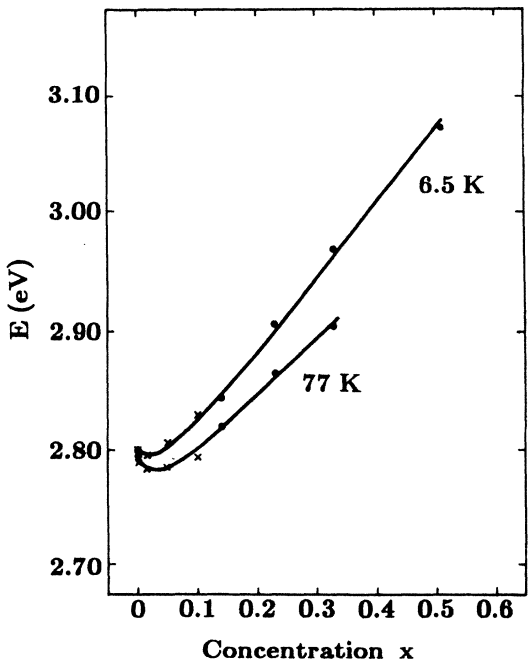

FIG. 6. PL peak energy of zinc-blende $Zn_{1-x}Mn_xSe$ as a function of Mn concentration x obtained by Twardowski *et al.* (Ref. 3) for bulk crystals (×) and by Kolodziejski *et al.* (Ref. 20) for MBE-grown epilayers (●). The lines are to guide the eye.

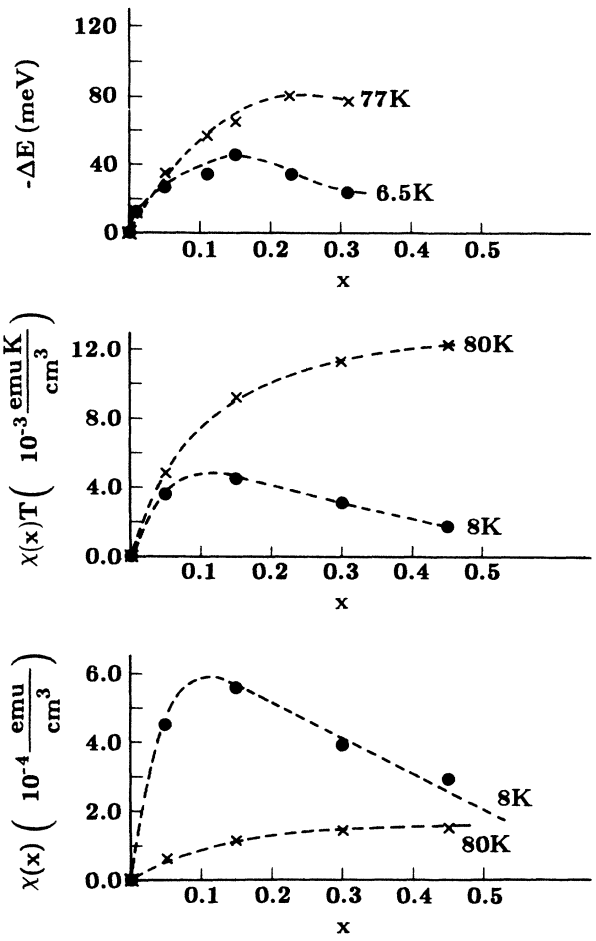

FIG. 7. Magnetic susceptibility χ, χT, and the nonlinear part of E_g-vs-x dependence ΔE (derived from data shown in Fig. 6) as a function of the concentration x. The lines are to guide the eye.

$E_{0g}(x,T)$ contains all the temperature and concentration dependence of the energy gap except for that due to the exchange interaction. Equation (9) predicts that the correction leads to a red shift of the band gap.

B. Analysis

To explain the band-gap closure with increasing x for $x<0.15$, we must estimate the amount of red shift of the band gap from our experimental data. This was done by assuming a linear dependence of E_{0g} on x and an extrapolated value of ~ 3.4 eV for the band gap on MnSe at 6.5 K. The energy shift ΔE was thus equal to $E_g(\mathrm{ZnSe})+Dx-E_{\mathrm{PL}}(x)$, with $D=0.6$ eV and E_{PL} our experimentally determined PL energy. To supplement our data and also to avoid the ambiguities occurring in the energy gap due to variations in crystal structure, the reflectivity results of Twardowski *et al.*[3] for $x \lesssim 0.103$ and results of PL measurements performed on MBE-grown zinc-blende $Zn_{1-x}Mn_xSe$ epilayers[20] ($0.15 \lesssim x \lesssim 0.51$) were used in this analysis (Fig. 6).

Equation (9) predicts a linear relationship between the quantity $\Delta E(x)$ and χT. Low-field magnetic susceptibility measurements have been made on various concentrations of $Zn_{1-x}Mn_xSe$.[26] These show that for all temperatures and concentrations $x \lesssim 0.30$, the spins exist in a paramagnetic phase, while for higher concentrations there is a transition to a spin-glass. The temperature of the transition depends on Mn concentration. (E.g., for $x=0.55$ the transition occurs at about 30 K). Thus, our use of a q-independent χ seems to be justified in the range of x of particular interest to us (i.e., in the region where anomalous closure of the band gap occurs, $x \lesssim 0.15$. Figure 7 shows the quantities $-\Delta E(x)$, χT, and χ for two temperatures plotted as a function of x. The 2.2- and 6.5-K results for E_g were used in conjunction with the 8-K susceptibility results because there is negligible variation of E_g with T in that temperature region. The susceptibility curve as a function of x exhibits a maximum at low T. This behavior has its origin in the antiferromagnetic coupling between the Mn spins, which tends to reduce the value of the susceptibility with growing x. This is because some of the Mn moments in the concentrated alloys compensate for each other and thus give no contribution to the susceptibility at T smaller than the characteristic energy of the Mn-Mn interaction. The 8-K results of χT and $-\Delta E$ both show a sharp rise for low x, a maximum between $x=0.10$ and 0.15, and then a decrease, while the 80-K values show an increase for low x and a leveling off for $x>0.25$. In the case of $-\Delta E(x)$, the concentration at which the values appear to decrease is dependent on the extrapolated value of the MnSe band gap used in computing $-\Delta E$. At any rate, the curves of $-\Delta E$ versus x and χT versus x exhibit the same

behaviors. A comparison of these two sets of data using the relation

$$E_g(x,T)=E_g(\mathrm{ZnSe})+Dx-b\chi T\ , \tag{10}$$

where the expression for b can be deduced from Eq. (9), gives $b=7.8$ eV cm^3/emu K. This corresponds to a $q_0\cong 3.3\times 10^7$ cm^{-1} (i.e., 0.3 of the Brillioun zone).

Next we consider the temperature dependence of E_g for the three different Mn concentrations measured by us. The behavior of the energy gaps of various semiconductors has been fitted by Varshni[4] to the equation

$$E_g(T)=E_0-\frac{AT^2}{T+B}\ . \tag{11}$$

ZnSe also follows this relation.[9] To this we have added the energy correction due to the exchange interaction, giving

$$E_g(x,T)=E_0+dx-\frac{AT^2}{T+B}-b\chi T\ . \tag{12}$$

Susceptibility data were available in the range 8 K $\leq T\leq$ 300 K for $x=0.05$, 0.30, and 0.45. The susceptibilities for $x=0.360$ and 0.554 were computed by interpolation using these data and the relation $\chi=(C_M x)/(T+\Theta x)$, which is valid for the paramagnetic region. $C_M x$ [$C_M=0.17$ (emu K/cm^3)] being the Curie constant and Θx ($\Theta=945$ K) the Curie-Wiess temperature, both of which can be obtained from the high-temperature susceptibility data for a sample with a given x value. The solid lines in Fig. 4 are fits using interpolated χ data and Eq. (12). The parameters used are listed in Table III. To reasonably fit the data, the values of b used were selected to be approximately four times smaller than that needed to reproduce the E_g versus x behavior. In view of the crudeness of the model and uncertainties in the material parameters this "order of magnitude" agreement can be regarded as quite satisfactory. The values for A and B are of a typical order of magnitude. They show a concentration dependence as well. As can be seen from the experimental data, there is a region of upward concavity in the E_g versus T curves for $x=0.360$ and 0.554. This cannot be reproduced by Eq. (12) and the available susceptibility data. This suggests that at higher Mn concentrations the theoretical description used is not complete. It is important to note that the onset of upward concavity occurs as the crystal is approaching a spin-glass phase. The assumptions used in our derivation were that (i) second-order effects were the dominant contribution to the band energy renormalization, (ii) the exchange parameters α,β were constant for $q\leq q_0$ and 0 for $q>q_0$, (iii) χ is independent of q, and (iv) the inelasticity of scattering could be neglected. In particular, it is quite possible that at high spin densities the energy correction is no longer proportional to χ and higher-order perturbation terms must be calculated. Also, the simplifying assumption that χ is q independent ceases to be valid as the spin-glass region is approached.[27]

TABLE III. Parameters obtained by fitting Eq. (12) to E_g vs T data of Fig. 3.

x	E_0 (eV)	A (K^{-1})	B (K)	b (eV cm^3/emu K)
0.066	2.805	0.000 62	200	2.0
0.360	3.007	0.000 80	100	2.0
0.554	3.144	0.000 90	75	1.6

VI. CONCLUSIONS

In conclusion, we have reported a systematic study of the band-edge PL as a function of concentration, together with a confirmation of reflectivity measurements. The data show that the band gap depends both on the Mn concentration and the crystal structure. The presence of polytypes in $Zn_{1-x}Mn_xSe$ was detected and used to explain the variation in E_g in the region of crystal structure transition. The value of the PL energy of hypothetical hexagonal MnSe was found to be $\sim$3.4 eV at 6.5 K. A shifting of the band-edge energies due to the exchange interaction of electrons in conduction and valence bands with the d electrons of the Mn was invoked to explain the minimum seen in E_g versus x. In particular, it is shown that there exists a correlation between the band-gap-versus-x variation and the magnetic susceptibility of the material, at least in the region where the anomalous decrease of E_g versus x is observed. It should be noted that this exchange-interaction-related modification of the band gap in the absence of applied magnetic field was particularly easy to observe in $Zn_{1-x}Mn_xSe$ because of the relatively small difference between E_g ($x=0$) and E_g ($x=1$), as compared to other DMS alloy systems. The temperature dependence of the energy gap for samples with $x>0.3$ shows an onset of upward concavity at $T\lesssim 150$ K (where the spin-glass phase is observed) which is unaccounted for in our model assuming q-independent χ. The magnetic susceptibility of such highly concentrated crystals is, however, a function of q.[27] Accounting for this dependence within the general framework of the model outlined in this paper may provide an explanation for the additional low-temperature blue shift, as argued by Diouri *et al.*[5] in the case of $Cd_{1-x}Mn_xTe$.

ACKNOWLEDGMENTS

The authors wish to thank Professor N. Otsuka for providing the transmission-electron-microscopy (TEM) measurements and determination of polytypes. We are also grateful to J. K. Furdyna for making susceptibility data available to us prior to publication and for a critical reading of the manuscript. This work has been supported in part by National Science Foundation (Materials Research Laboratories Program) under Grant No. DMR-83-16988.

*On leave from Institute of Physics, Polish Academy of Sciences, PL-02-668 Warsaw, Poland.

[1]J. K. Furdyna, J. Appl. Phys. **53**, 7637 (1982); N. B. Brandt and V. V. Moshchkalkov, Adv. Phys. **33**, 193 (1984).

[2]D. Yoder-Short, Y. Debska, and J. K. Furdyna, J. Appl. Phys. **58**, 4056 (1985).

[3]A. Twardowski, T. Dietl, and M. Demianiuk, Solid State Commun. **48**, 845 (1983).

[4]Y. P. Varshni, Physica **34**, 149 (1967).

[5]J. Diouri, J. P. Lascaray, and M. El Amrani, Phys. Rev. B **31**, 7795 (1985).

[6]J. E. Morales-Toro, W. M. Becker, B. I. Wang, and U. Debska, Solid State Commun. **52**, 41 (1984).

[7]J. E. Morales, W. M. Becker, and U. Debska, Phys. Rev. B **32**, 5202 (1985).

[8]A. Pajaczkowska, Prog. Cryst. Growth Charact. **1**, 289 (1978).

[9]P. J. Dean and J. L. Merz, Phys. Rev. **178**, 1310 (1968).

[10]Y. Shirakawa and H. Kukimoto, J. Appl. Phys. **51**, 2014 (1980).

[11]P. J. Dean, D. C. Herrbert, C. J. Werkhoven, B. J. Fitzpatrick, and R. N. Bhargava, Phys. Rev. B **23**, 4888 (1981).

[12]J. L. Merz, K. Nassau, and J. W. Shiever, Phys. Rev. B **8**, 1444 (1973).

[13]M. Glicksman and W. D. Kraeft, Solid-State Electron. **28**, 151 (1985).

[14]G. E. Hite, D. T. F. Marple, M. Aven, and B. Segall, Phys. Rev. **156**, 850 (1966).

[15]J. E. Morales (private communication).

[16]O. Brafman and I. T. Steinberger, Phys. Rev. **143**, 501 (1966).

[17]J. L. Birman, Phys. Rev. **115**, 1493 (1959).

[18]See, *Landolt-Börnstein Table,* Vol. 17b of *New Series Group III,* edited by O. Madelung, M. Schulz, and H. Weiss (Springer-Verlag, Berlin, 1983), p. 142.

[19]J. Stankiewicz, Phys. Rev. B **27**, 3631 (1983).

[20]L. A. Kolodziejski, R. L. Gunshor, R. Venkatasubramanian, T. C. Bonsett, R. Frohne, S. Datta, N. Otsuka, R. B. Bylsma, W. M. Becker, and A. V. Nurmikko, J. Vac. Sci. Technol. B **4**, 583 (1986).

[21]M. Ikeda, K. Itoh, and H. Sato, J. Phys. Soc. Jpn. **25**, 455 (1968).

[22]D. Heiman, Y. Shapira, and S. Foner, Solid State Commun. **51**, 603 (1984).

[23]F. Rys, J. S. Helman, and W. Baltensperger, Phys. Kondens. Mater. **6**, 105 (1967).

[24]C. Haas, Phys. Rev. **168**, 531 (1968).

[25]J. A. Gaj, J. Ginter, and R. R. Galazka, Phys. Status Solidi B **89**, 655 (1978).

[26]J. K. Furdyna, R. B. Frankel, and U. Debska (unpublished).

[27]T. M. Holden, G. Doling, V. F. Sears, J. K. Furdyna, and W. Giriat, Phys. Rev. B **26**, 5074 (1982).